A. Supplementary Material – Chapter 2

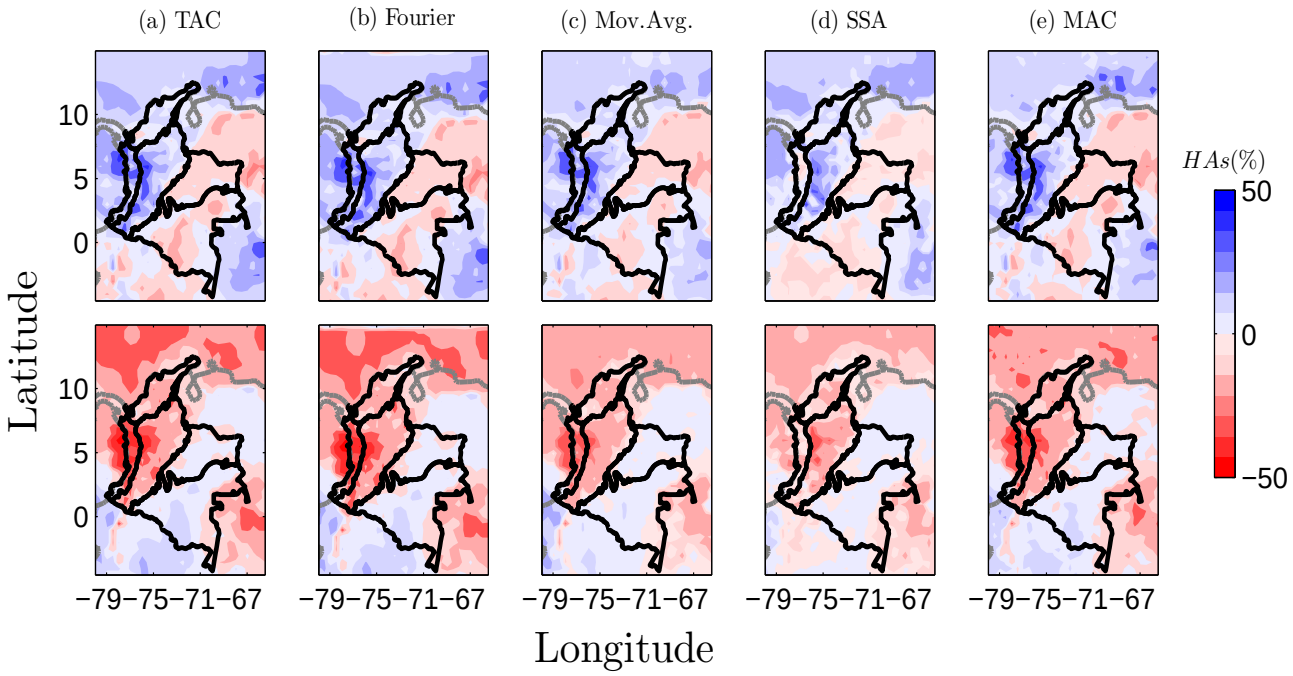

Figures A-1.: Composite rainfall anomalies (HAs) over Colombia (Dataset No. 1), during ENSO, estimated by the five HAs methods. (Top panels) HAs during La Niña (LN). (Bottom panels) HAs during El Niño (EN). (dark line) boundaries of the natural regions of Colombia. (gray line) northern South America boundaries of countries. The classification of ENSO events was done using the ONI index.

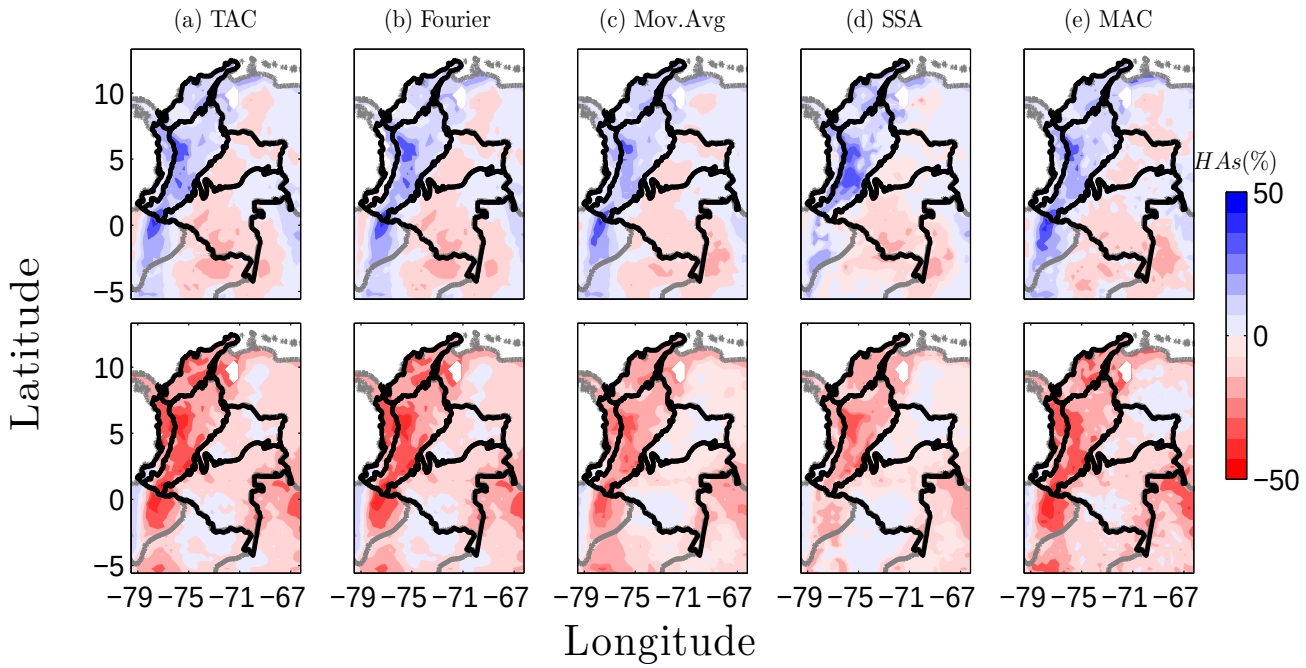

Figures A-2.: Composite rainfall anomalies (HAs) over Colombia (Dataset No. 2), during ENSO, estimated by the five HAs methods. (Top panels) HAs during La Niña (LN). (Bottom panels) HAs during El Niño (EN). (dark line) boundaries of the natural regions of Colombia. (gray line) northern South America boundaries of countries. The classification of ENSO events was done using the ONI index.

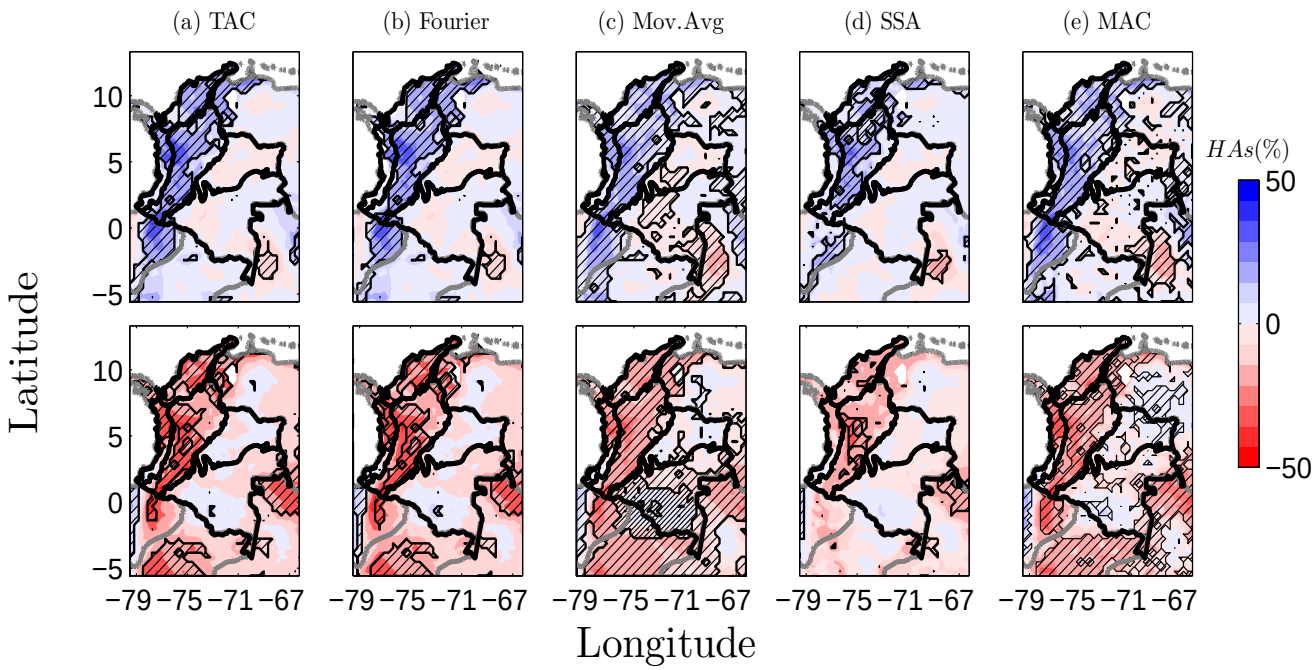

Figures A-3.: Composite analysis for rainfall anomalies (Dataset No. 2) showing the zones where mean anomalies for La Niña (top row) and El Niño (bottom row) are statistically different to the mean anomalies for the neutral phases of ENSO. (hatched lines) zones of statistically different mean values using the t-test at the 0.05 significance level. The classification of the ENSO events was done using the MEI index.

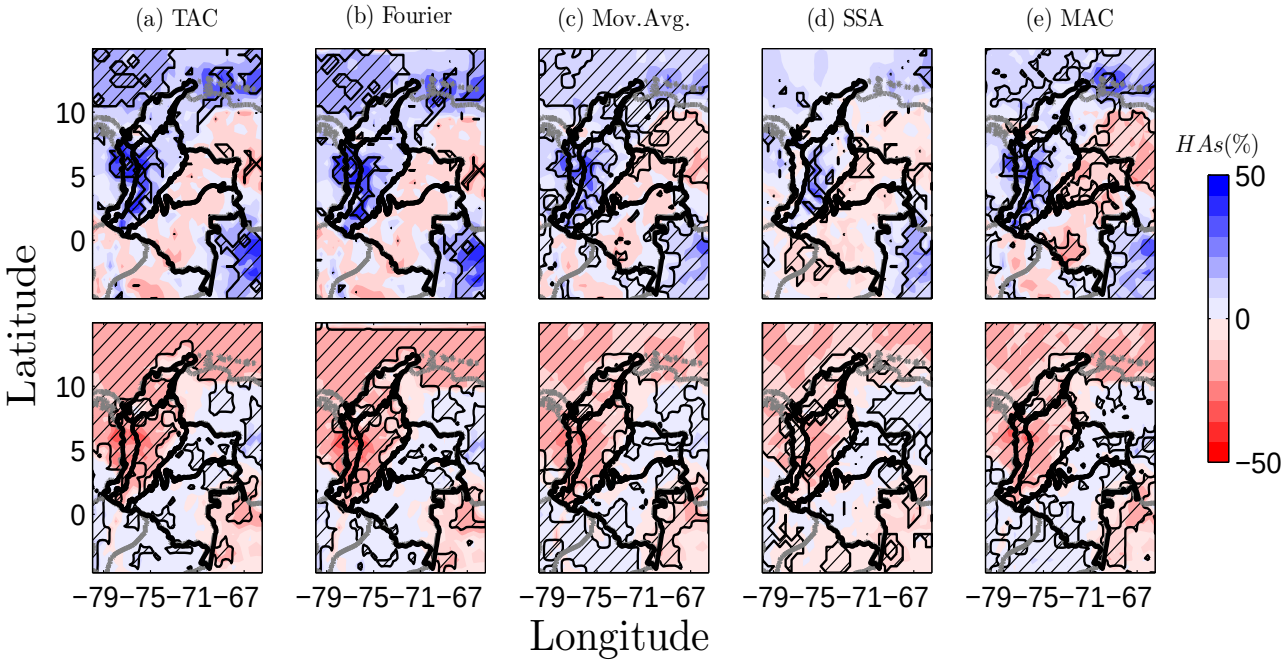

Figures A-4.: Composite analysis for rainfall anomalies (Dataset No. 1) showing the zones where mean anomalies for La Niña (top row) and El Niño (bottom row) are statistically different to the mean anomalies for the neutral phases of ENSO. (hatched lines) zones of statistically different mean values using the Terray's test at the 0.05 significance level. The classification of the ENSO events was done using the MEI index.

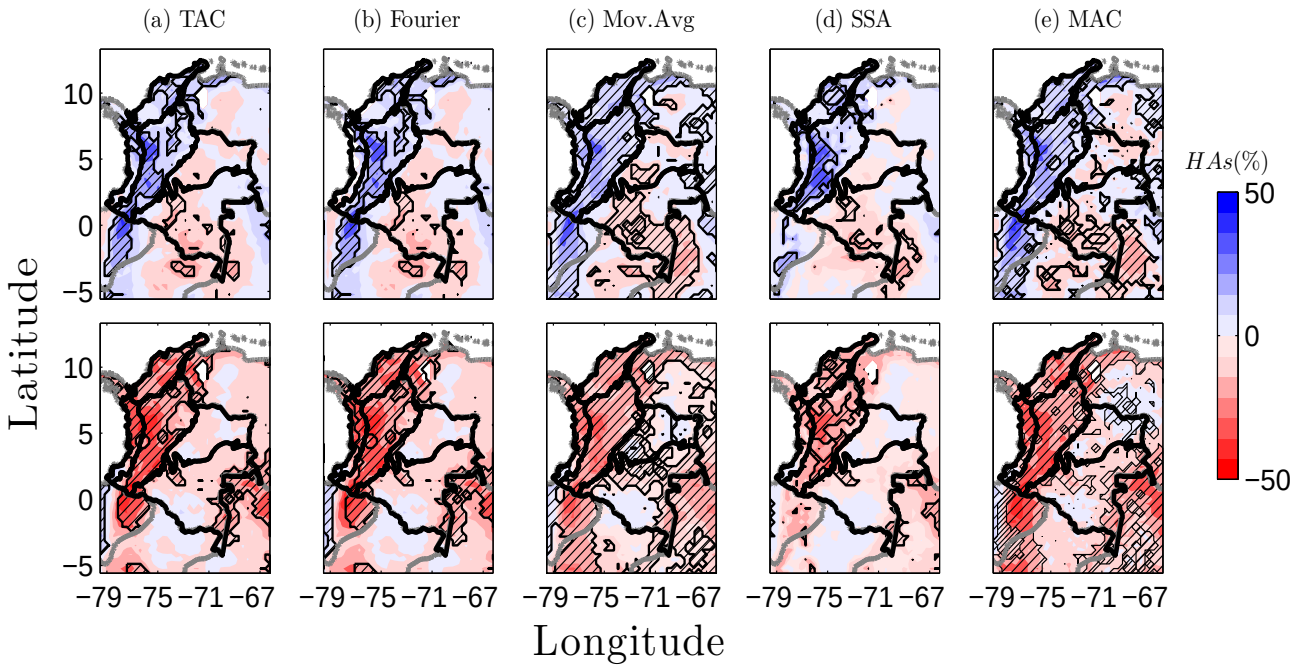

Figures A-5.: Composite analysis for rainfall anomalies (Dataset No. 2) showing the zones where mean anomalies for La Niña (top row) and El Niño (bottom row) are statistically different to the mean anomalies for the neutral phases of ENSO. (hatched lines) zones of statistically different mean values using the t-test at the 0.05 significance level. The classification of the ENSO events was done using the ONI index.

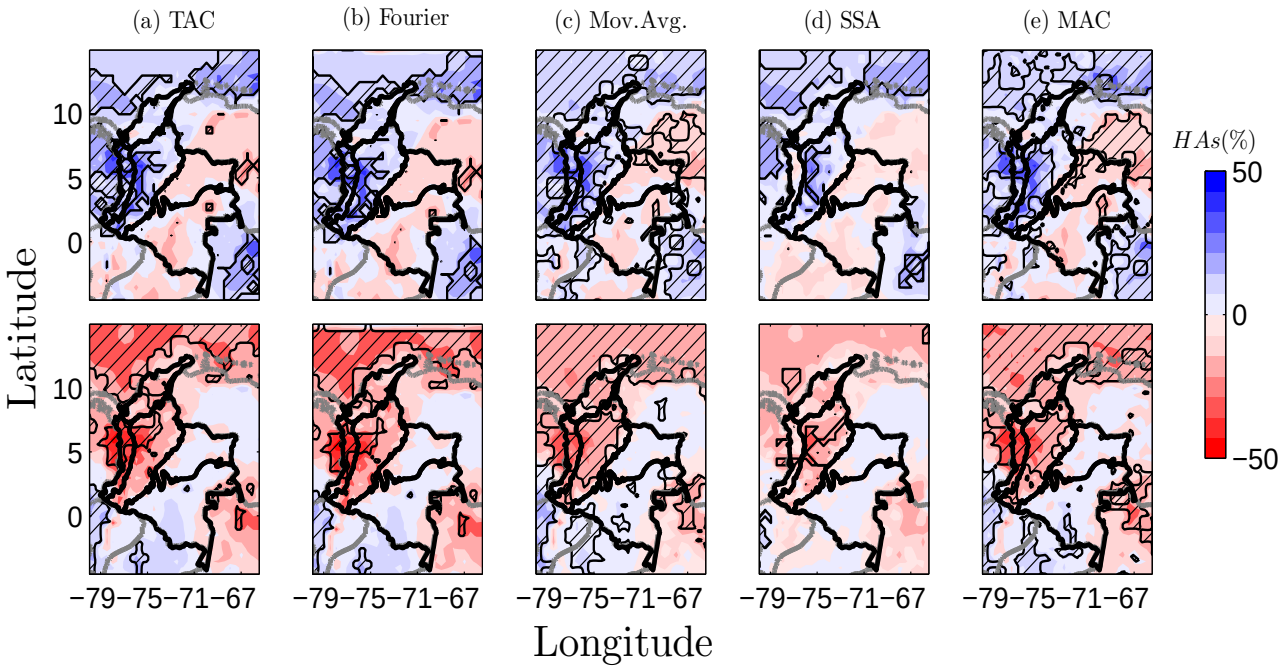

Figures A-6.: Composite analysis for rainfall anomalies (Dataset No. 1) showing the zones where mean anomalies for La Niña (top row) and El Niño (bottom row) are statistically different to the mean anomalies for the neutral phases of ENSO. (hatched lines) zones of statistically different mean values using the t-test at the 0.05 significance level. The classification of the ENSO events was done using the ONI index.

B. Supplementary Material – Chapter 3

This Supplementary Information provides details that are not included in the body of Chapter 3. It includes information on the pre-processing of data before the Phase Synchronization (PS) analysis, Fourier periodograms, size of data-sets according to the ENSO classification for El Niño and La Niña, Annual Cycles of precipitation for the regions of Colombia, PS functions, maps of PS, and anomalies.

B.1. Pre-processing data: Filtering and Definition of HyAns

In general, quantify phase interactions between the ENSO signal and the AC and anomalies of the hydrological variables in Colombia requires the following series of steps: *(i)* to define representative time series for the regions of Colombia, *(ii)* to standardize data (without subtract the seasonal variability), *(iii)* to filter out data in order to define the AC, high-frequencies and noise of the hydrological variables as well as their anomalies in relation to the AC, *(iv)* to test the significance of frequencies at seasonal timescales in the anomalies time series and, *(v)* to test the significance of the PS metrics. Hence, the detailed steps behind our PS analysis are described as follow:

- **Step 1:** From our precipitation data set No. 1 of monthly Precipitation fields in Colombian territory hurtado14, we obtain the average monthly time series for each natural region for the period 1975-2006. The same procedure is carried out for data set No. 2 (IDEAM time series), averaging precipitation for the natural regions for the period 1976-2015.

- **Step 2:** The time series are standardized by subtracting the long-term average (grand-mean) and dividing by the long-term standard deviation (grand-standard deviation). Then, the standardized hydrological variables conserve their annual variability although the new series have zero mean and unit standard deviation. Hence, this standardization process does not remove the annual cycle.

- **Step 3:** Each time series is filtered using EEMD to obtain signals at the frequency band of the AC (hereafter MAC time series). Due to significant semi-annual (6 months) and annual (12 months) periodicities in data for the different regions of Colombia (see

Fig. **B-1**), MAC time series include both the annual and semi-annual signals, which explain more than 70% of total variance (Table **B-2**).

- **Step 4:** To test the significance of residual frequencies at seasonal timescales (6 months and 12 months) in the time series of anomalies, using the test proposed by [*Ahdesmäki, et al.*(2005)] ($\alpha = 0.05$). In this step, we aim to avoid biases in the long-term characterization of regional anomalies due to the presence of significant seasonal frequencies in time series.

- **Step 5:** To calculate the anomalies of precipitation and streamflows by EEMD filtering and to subtract the MAC from the time series obtained in Step 2. Then, the residual data after subtracting MAC are denoted as total anomalies, A_T. The intra-annual frequencies of A_T are denoted high-frequency anomalies, A_{HF}, and the inter-annual frequencies of A_T are denoted low-frequency anomalies, A_{LF}. In general, hydro-climatic anomalies are presented as standardized anomalies with the standard deviation of each month from the original time series as scale factor. Figure **B-2** illustrates the MAC in relation to the original signal (panel a) as well as the total rainfall anomalies, A_T (including noise and intra-annual frequencies), and Low-frequency anomalies, A_{LF}.

- **Step 6:** The SST3.4 time series is filtered out using EEMD to obtain the inter-annual frequency bands and avoid the presence of seasonal residuals associated with the annual cycle. Fig. **B-3** shows that the original SST3.4 time series contains significant seasonal components (6 and 12 months) whereas in the filtered SST3.4 they are no longer present, according to the test by [*Ahdesmäki, et al.*(2005)], at the significance level $\alpha = 0.05$.

- **Step 7:** The filtered SST3.4 signal, the MAC and anomalies time series are compared using the GPD method in combination with the SPS estimator. The PS analysis is carry out according to El Niño and La Niña states of ENSO.

- **Step 8:** Possible time-lags between ENSO signal and the Colombian hydrology phase time series are evaluated using the Phase-Lag estimator.

- **Step 9:** The significance of the strength of phase synchronization, χ, is assessed using the significance test presented in the body of the article.

Tables B-1.: Data points according to ENSO's states for each dataset.

		Total monthly data points			Average data points per mont		
Datasets	**Period**	**El Niño**	**La Niña**	**Neutral**	**El Niño**	**La Niña**	**Neutra**
Hurtado & Mesa (2014)	1975-2006	158	65	161	13[10 – 15]	5[3 – 10]	13[10 – 1
IDEAM–Precipitation	1976-2015	193	85	202	16[12 – 19]	7[2 – 13]	16[12 – 2
IDEAM–Streamflows	1976-2013	176	85	195	14[11 – 17]	7[2 – 13]	16[11 – 2
XM–Streamflows	1976-2015	193	85	202	16[12 – 19]	7[2 – 13]	16[12 – 2

Tables B-2.: Percentage of the total variance, σ^2, explained by the MAC; Total Anomalies,A_T (in relation to MAC); Low-Frequency Anomalies, A_{LF}, and High-Frequency Anomalies,A_{HF}. Dataset [*Hurtado and Mesa*(2014)].

Region	% σ^2 **MAC**	% σ^2 A_T	% σ^2 A_{HF}	% σ^2 A_{LF}
Andean	85.16	14.84	6.87	7.96
Caribbean	85.77	14.23	5.10	9.13
Pacific	72.63	27.37	16.27	11.10
Orinoco	92.66	7.34	1.59	5.74
Amazon	72.82	27.18	8.67	18.52

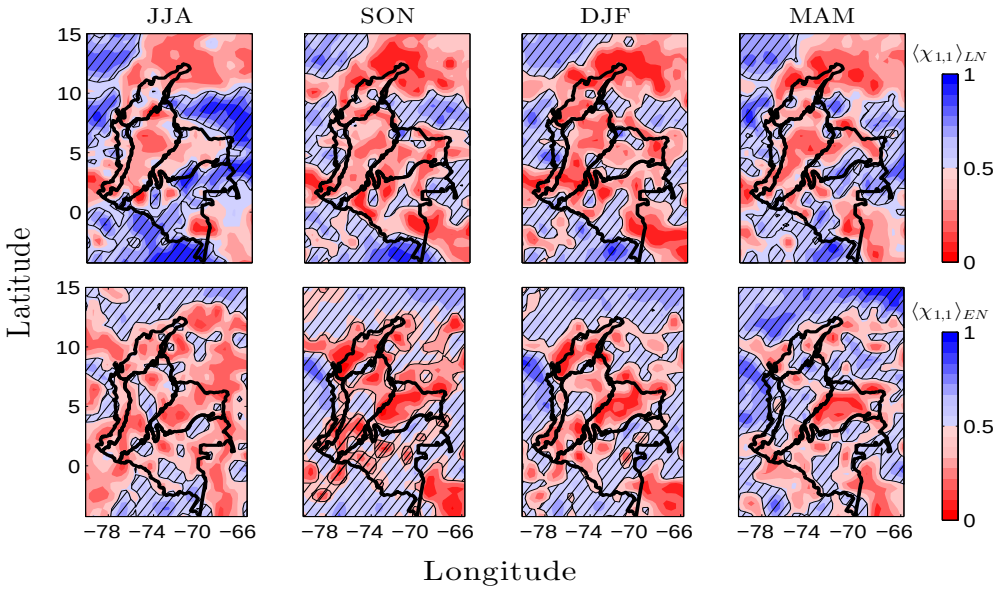

Figures B-16.: Strength of phase synchronization, $\langle\chi\rangle$, between the AMO index and rainfall anomalies in Colombia during ENSO. Phase ratio $\Phi_{1,1}$, Data set No. 1. (top row) La Niña $\langle\chi\rangle_{LN}$. (bottom row) El Niño $\langle\chi\rangle_{EN}$. The hatched contours indicate zones where χ is significant at 5%.

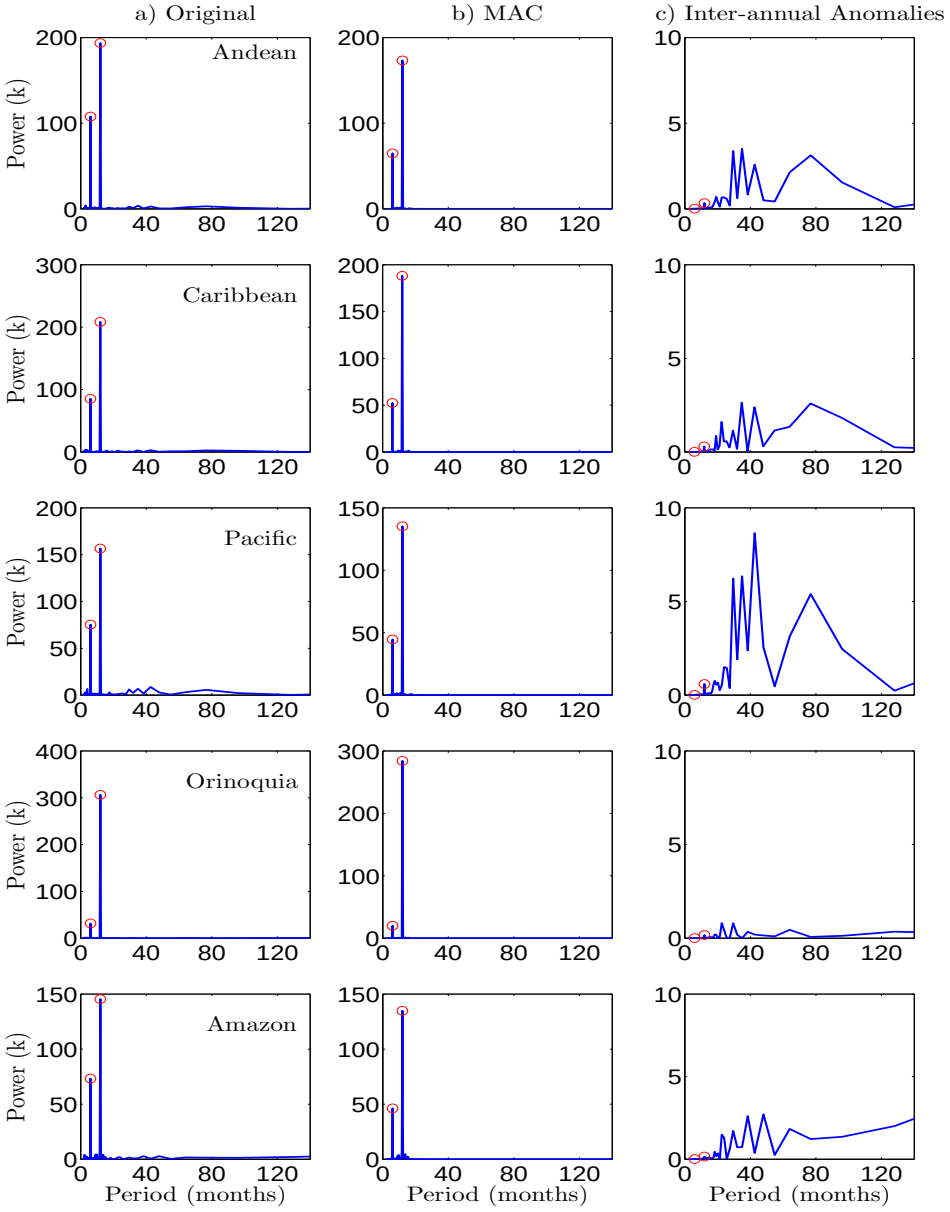

Figures B-1.: Periodogram for average precipitation in Colombian regions (Data set No. 1). a) Original data, b) Modulated Annual Cycle (MAC) and c) Low-frequency anomalies, A_{LF}, filtered out using EEMD. Red circles indicate peaks at seasonal time-scales.

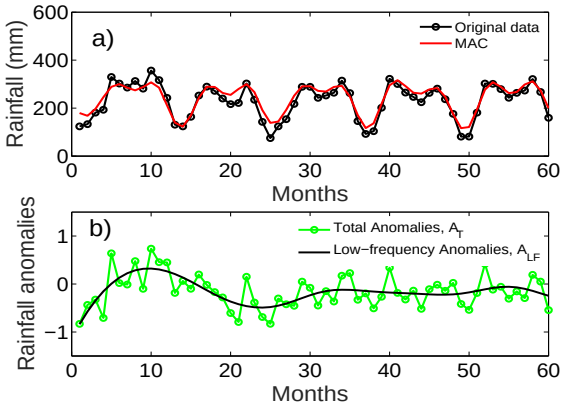

Figures B-2.: Time series of rainfall and its standardized anomalies in the Andean region (Data set No. 1), example for a 5 years record length. a) Original averaged time series and its MAC. b) Rainfall anomalies after subtracting MAC or total anomalies, A_T and low-frequency anomalies or anomalies at inter-annual scales, A_{LF}.

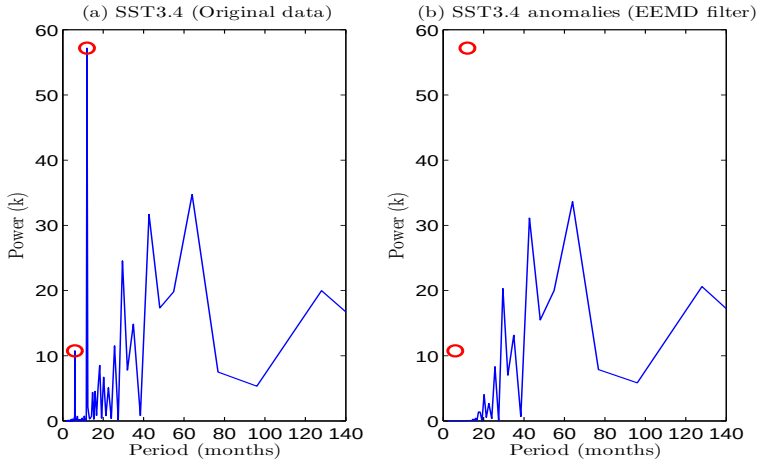

Figures B-3.: Periodogram (a) Original MEI index data and (b) MEI index filtered using EEMD to eliminate seasonal residual frequencies. Red circles indicates change in a frequency peak.

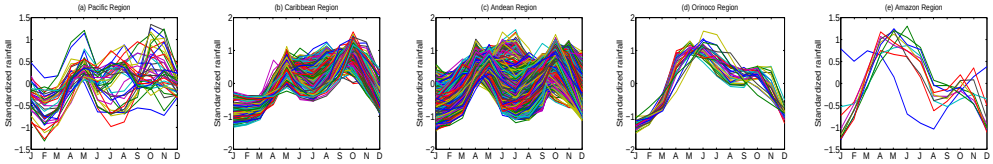

Figures B-4.: Annual cycle of precipitation for each region of Colombia (Data set No. 2) using standardized data (including their AC). i.e. for subtracting from each time series its grand-mean and dividing by its grand-standard deviation

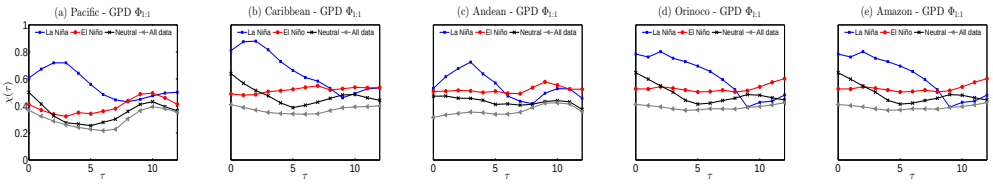

Figures B-5.: Strength of phase synchronization, χ, between ERSST3.4 and long-term mean regional precipitation (both time series containing their annual cycles), using the Data set No. 2, with $\Phi_{1,1}$. (a-e) χ as a function of lag τ (in months) for El Niño and La Niña.

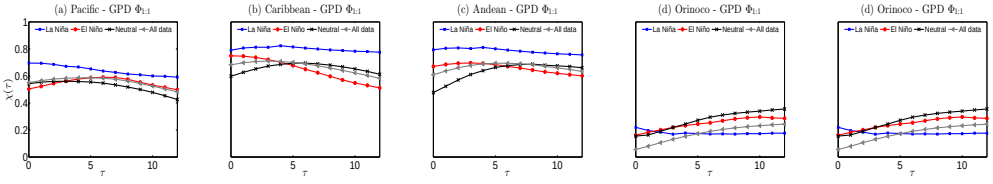

Figures B-6.: Strength of phase synchronization, χ, between the SST34 anomalies and the standardized rainfall anomalies, A_{LF}. (Data set No. 2; 1976-2015) with $\Phi_{1,1}$. (a-c) χ as a function of lag τ (in months) for El Niño and La Niña.

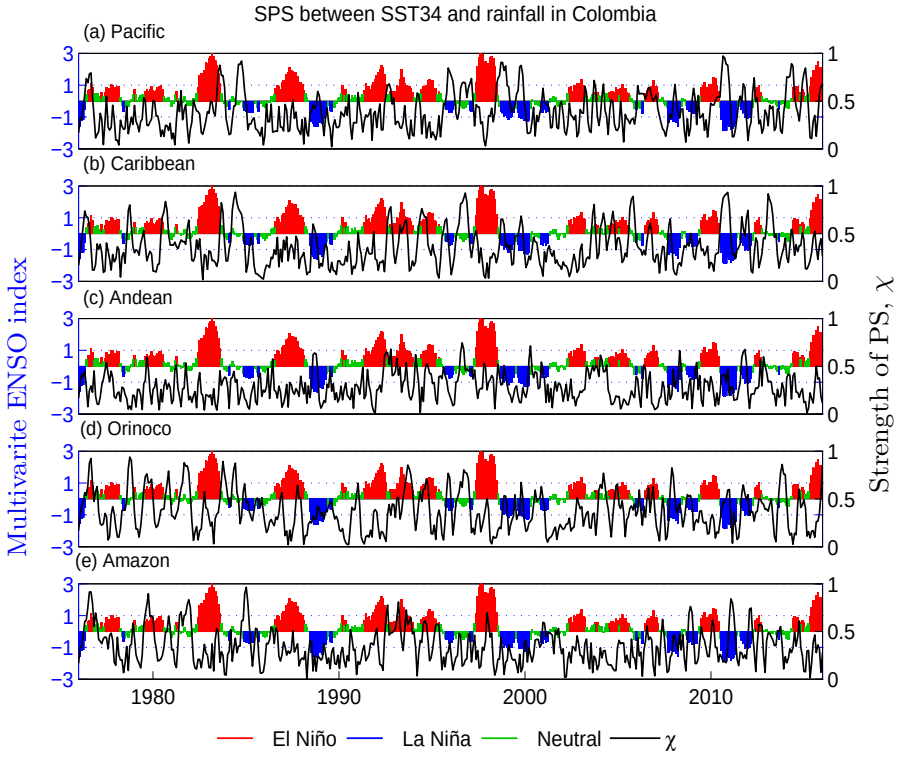

Figures B-7.: Strength of phase synchronization between ERSST3.4 and long-term mean regional precipitation (both time series containing their annual cycles), using the Data set No. 2 (1976-2015), with $\Phi_{1,1}$. [left axis] Multivariate ENSO index indicating periods El Niño, La Niña, and Neutral. [right axis] Strength of PS, χ

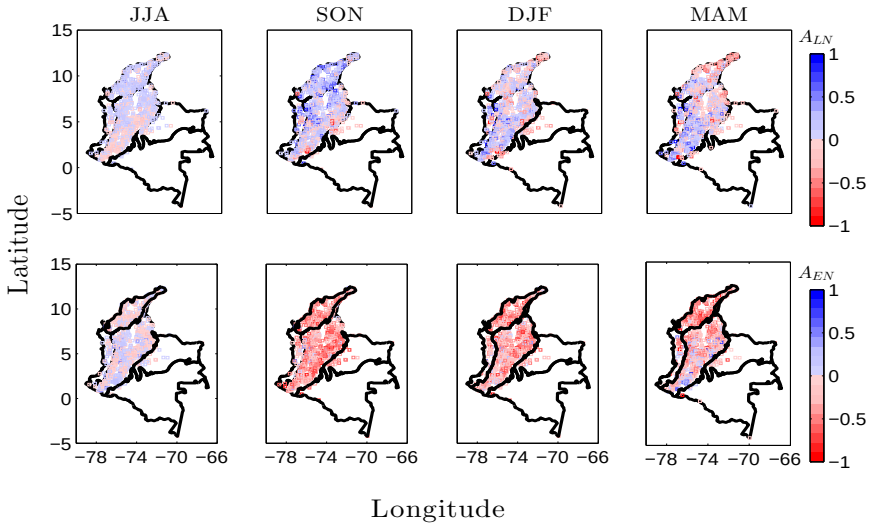

Figures B-8.: Seasonal average composite rainfall anomalies (HyAns) over Colombia, during ENSO (Data set No. 2), period 1976-2006. (Top panels) HyAns during La Niña (A_{LN}). (Bottom panels) HyAns during El Niño (A_{EN}).

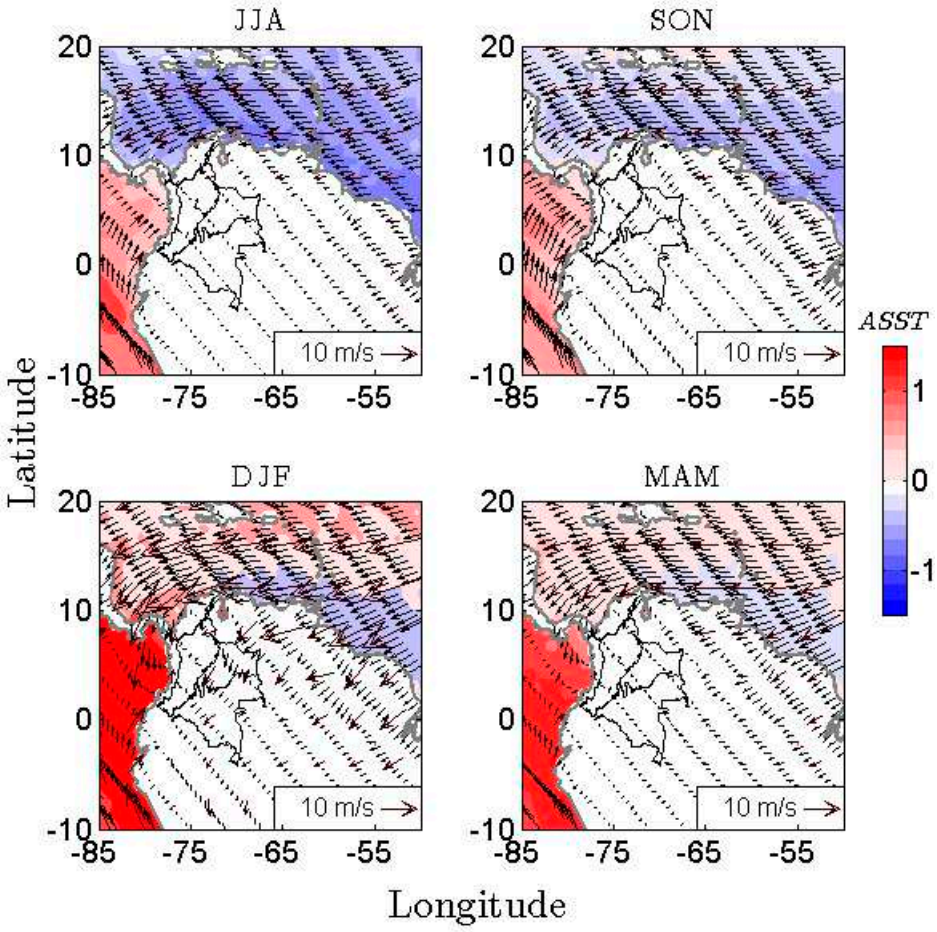

Figures B-9.: Composite of anomalies of sea surface temperatures (ASST) during El Niño. (arrows) climatology of winds during El Niño for the period 1979-2018 using ERA5.

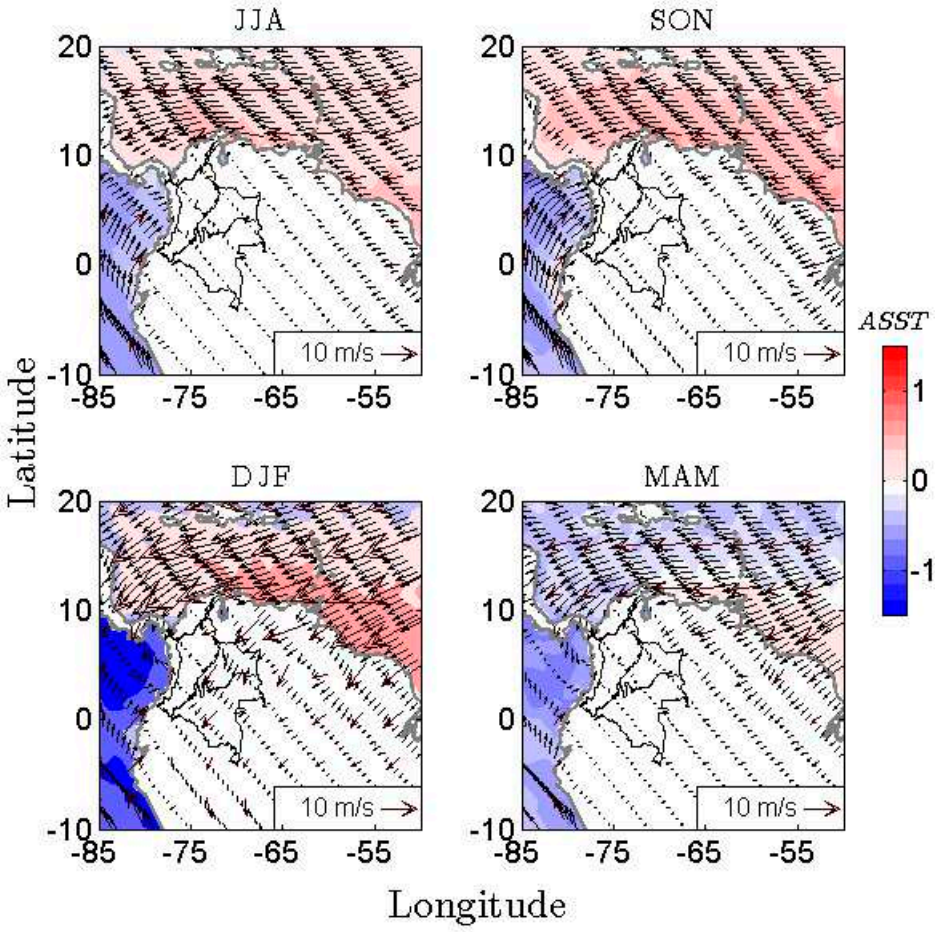

Figures B-10.: Composite of anomalies of sea surface temperatures (ASST) during La Niña. (arrows) climatology of winds during La Niña for the period 1979-2018 using ERA5.

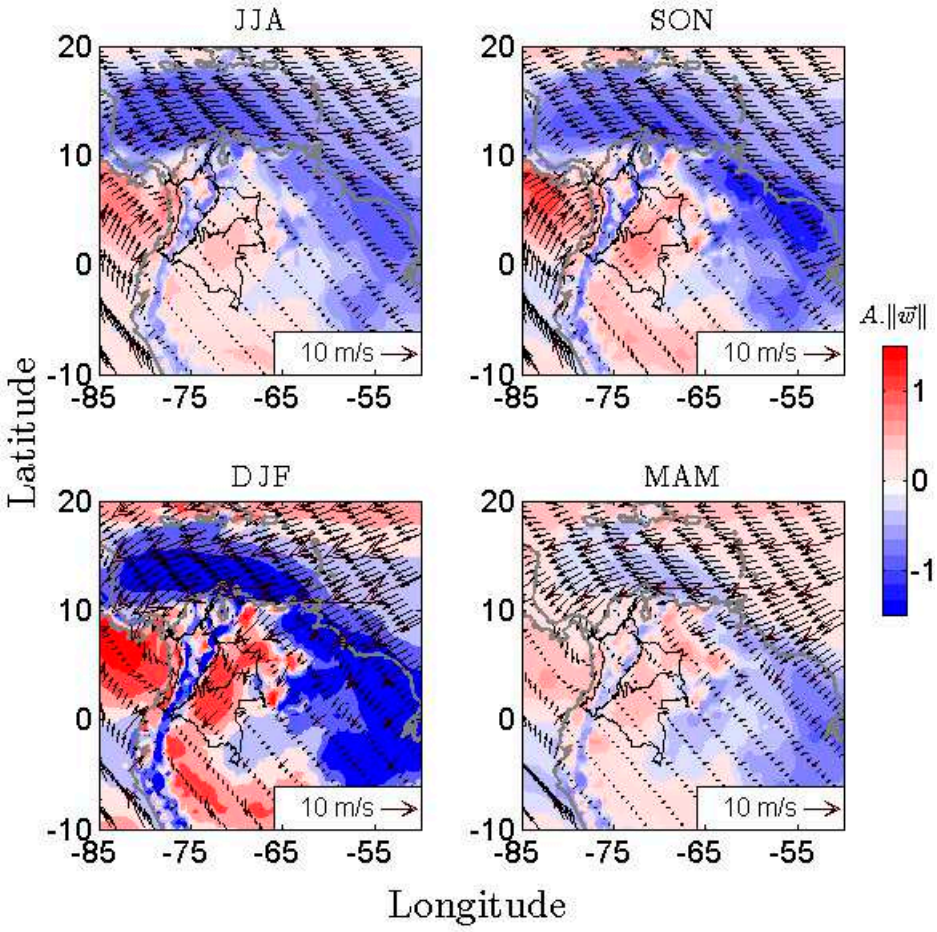

Figures B-11.: Composite of anomalies of the surface winds magnitude at 100m ($A \cdot \|\overrightarrow{w}\|$) during La Niña. (arrows) climatology of winds during La Niña for the period 1979-2018 using ERA5.

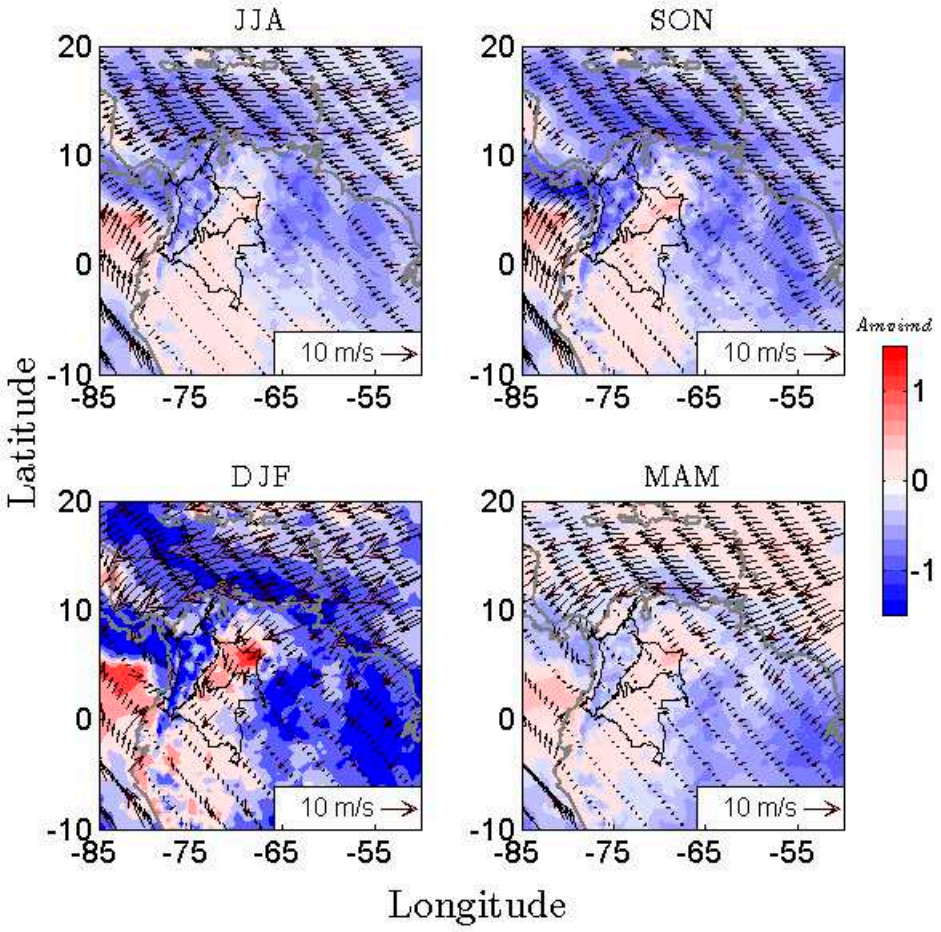

Figures B-12.: Composite of mean vertical integrated moisture divergence (*Amvimd*) during La Niña. (arrows) climatology of winds during La Niña for the period 1979-2018 using ERA5.

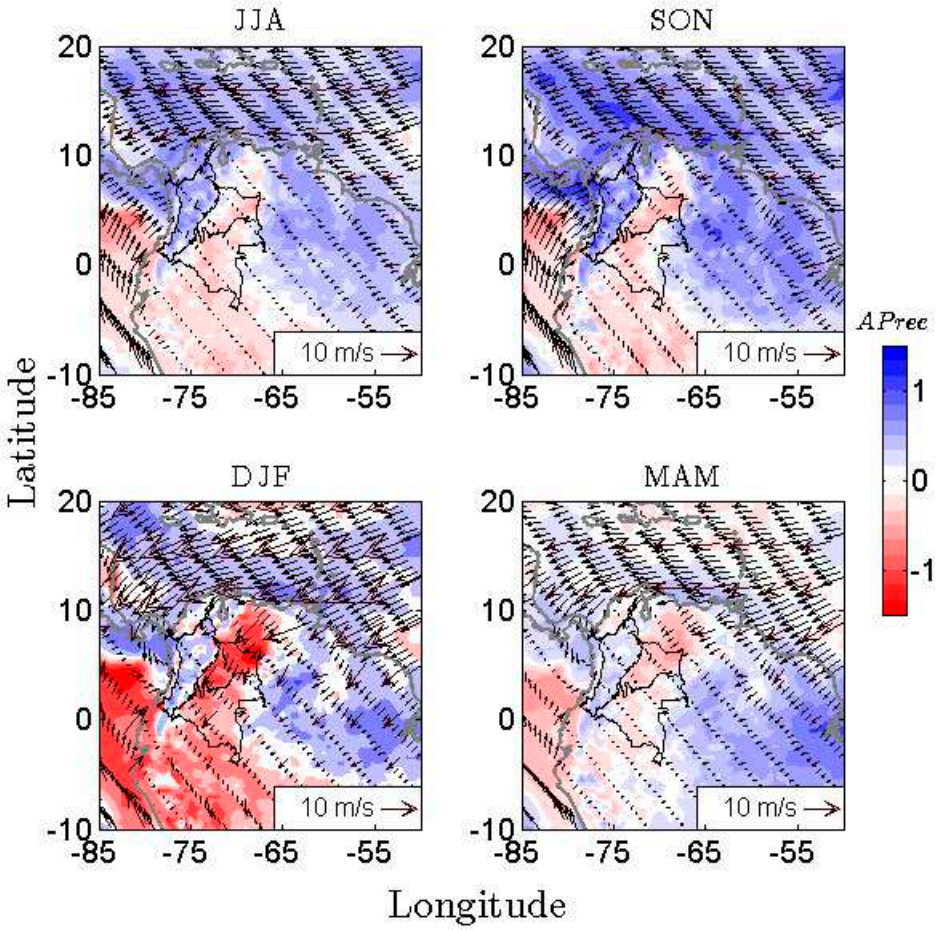

Figures B-13.: Composite of rainfall anomalies ($APrec$) during La Niña. (arrows) climatology of winds during La Niña for the period 1979-2018 using ERA5.

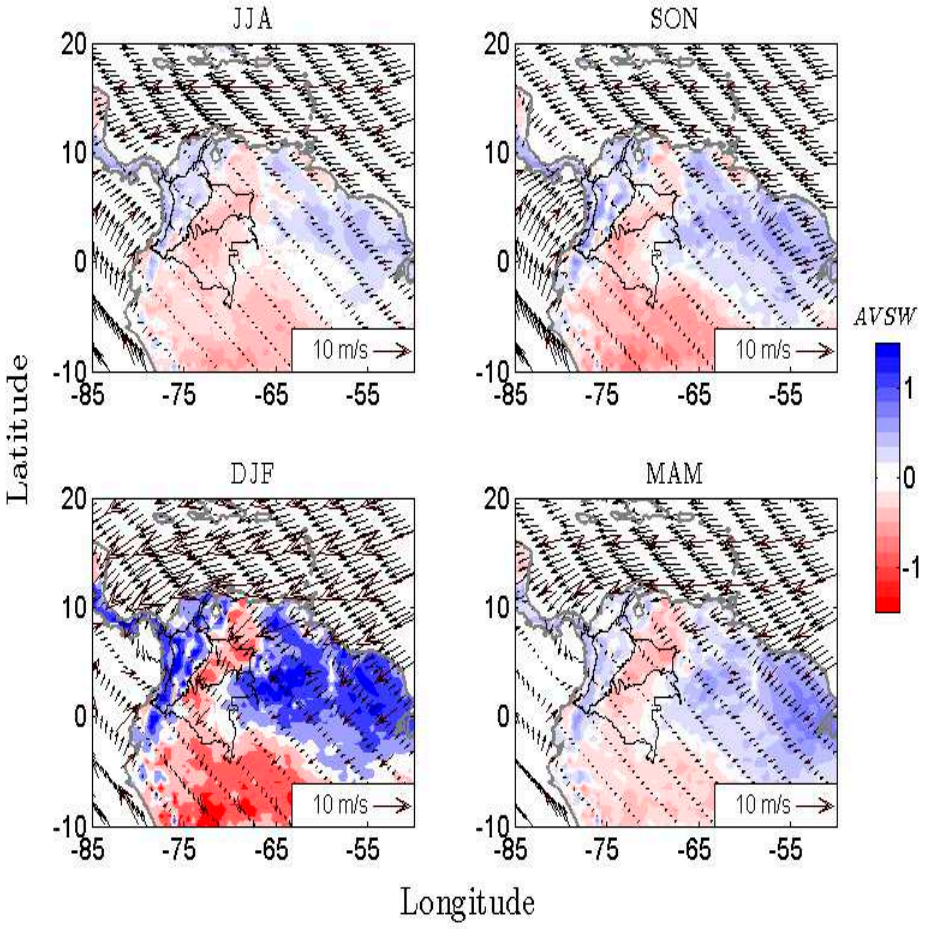

Figures B-14.: Composite of volumetric soil water anomalies (AVSW) during La Niña. (arrows) climatology of winds during La Niña for the period 1979-2018 using ERA5.

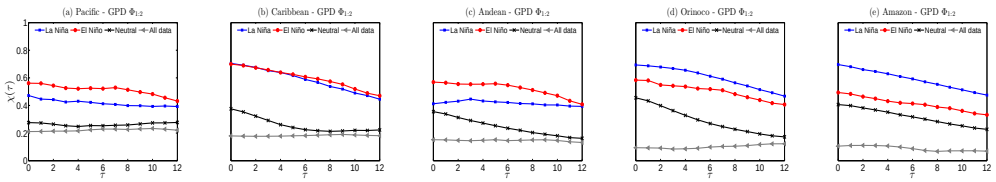

Figures B-15.: Strength of phase synchronization, χ, between the SST34 anomalies and the MAC of rainfall. (Data set No. 2; 1976-2015) with $\Phi_{1,2}$. (a-c) χ as a function of lag τ (in months) for El Niño and La Niña.

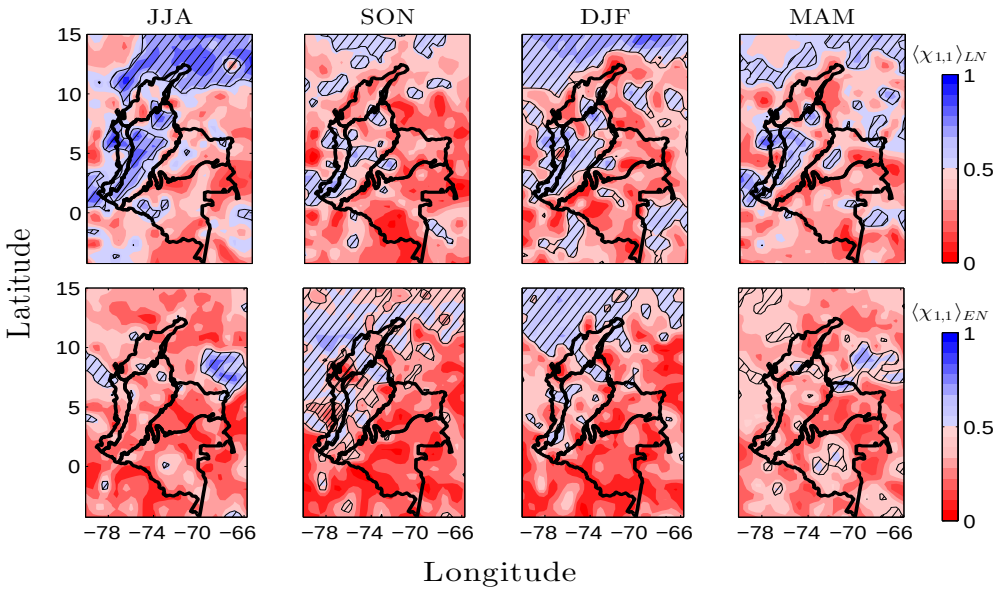

Figures B-17.: Strength of phase synchronization, $\langle\chi\rangle$, between the TNA index and rainfall anomalies in Colombia during ENSO. Phase ratio $\Phi_{1,1}$, Data set No. 1. (top row) La Niña $\langle\chi\rangle_{LN}$. (bottom row) El Niño $\langle\chi\rangle_{EN}$. The hatched contours indicate zones where χ is significant at 5%.

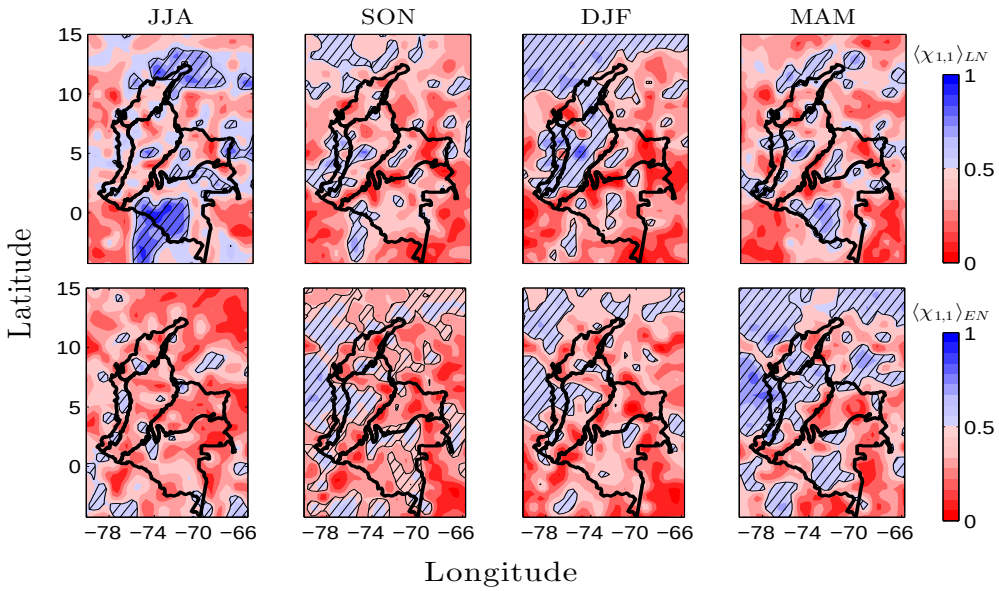

Figures B-18.: Strength of phase synchronization, $\langle\chi\rangle$, between the CAR index and rainfall anomalies in Colombia during ENSO. Phase ratio $\Phi_{1,1}$, Data set No. 1. (top row) La Niña $\langle\chi\rangle_{LN}$. (bottom row) El Niño $\langle\chi\rangle_{EN}$. The hatched contours indicate zones where χ is significant at 5%.

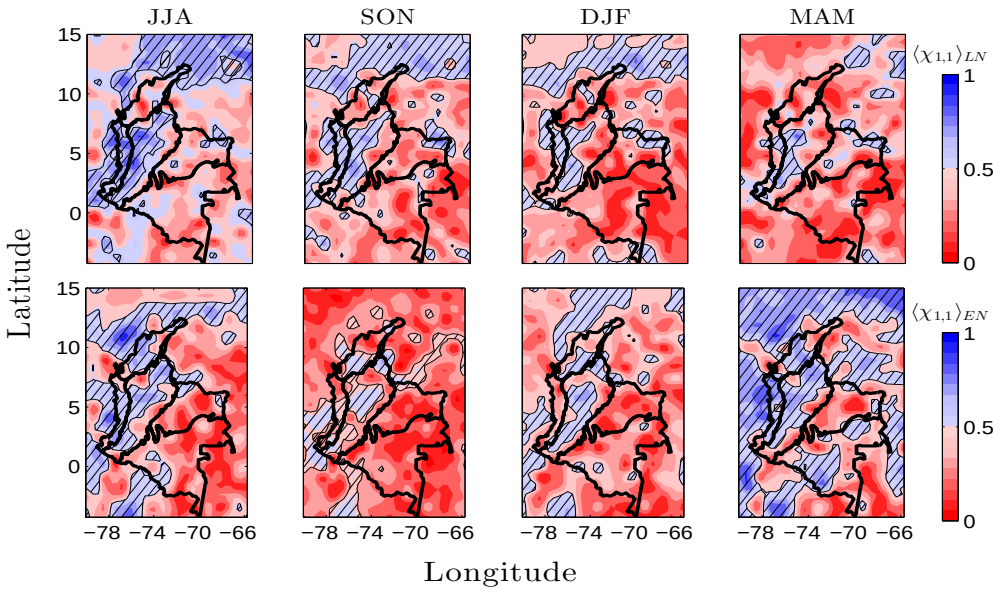

Figures B-19.: Strength of phase synchronization, $\langle\chi\rangle$, between the SST anomalies in the N12 zone and rainfall anomalies in Colombia during ENSO. Phase ratio $\Phi_{1,1}$, Data set No. 1. (top row) La Niña $\langle\chi\rangle_{LN}$. (bottom row) El Niño $\langle\chi\rangle_{EN}$. The hatched contours indicate zones where χ is significant at 5%.

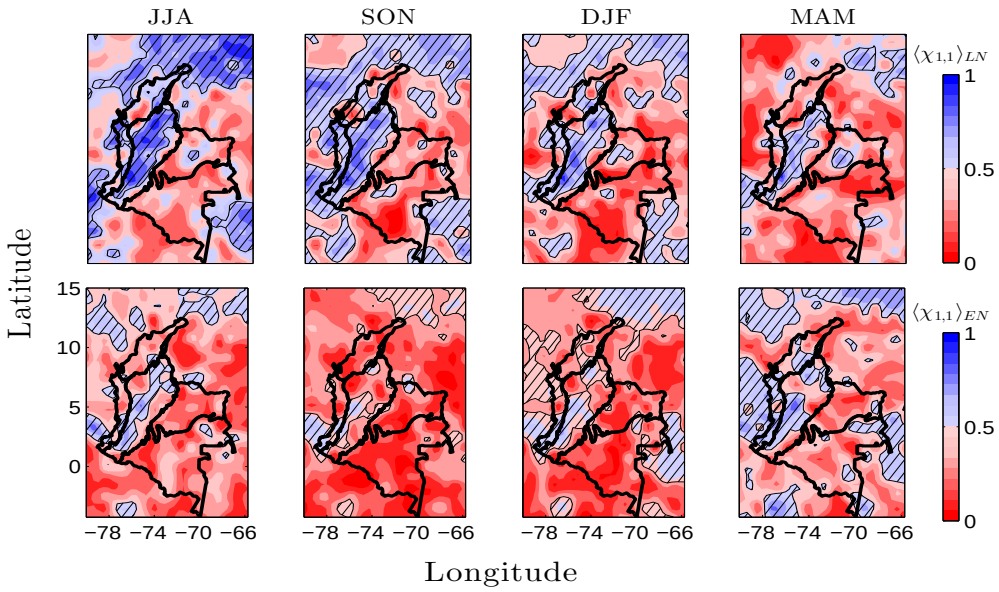

Figures B-20.: Strength of phase synchronization, $\langle\chi\rangle$, between the MEI index and rainfall anomalies in Colombia during ENSO. Phase ratio $\Phi_{1,1}$, Data set No. 1. (top row) La Niña $\langle\chi\rangle_{LN}$. (bottom row) El Niño $\langle\chi\rangle_{EN}$. The hatched contours indicate zones where χ is significant at 5%.

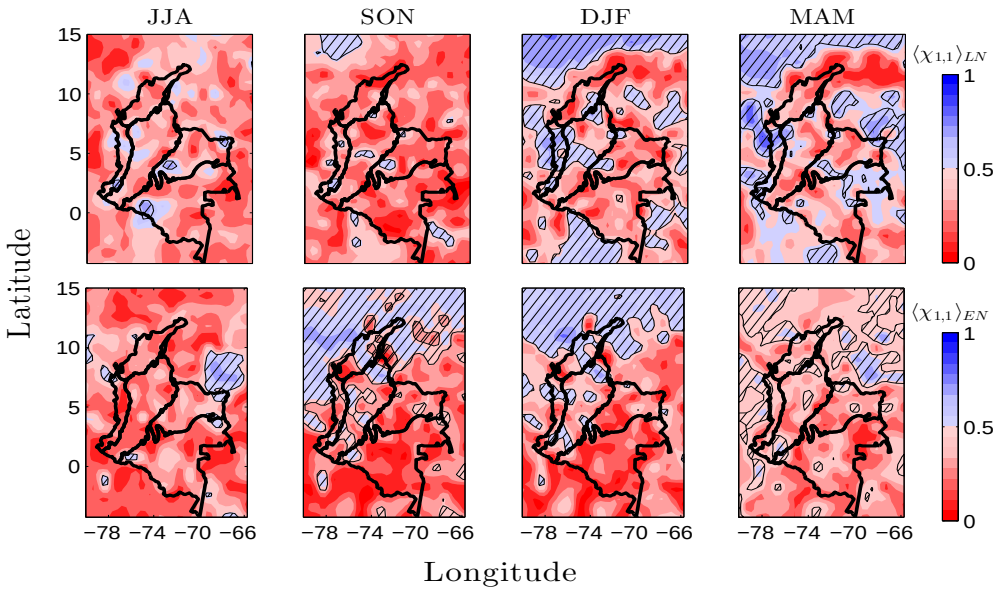

Figures B-21.: Strength of phase synchronization, $\langle\chi\rangle$, between the AMM index and rainfall anomalies in Colombia during ENSO. Phase ratio $\Phi_{1,1}$, Data set No. 1. (top row) La Niña $\langle\chi\rangle_{LN}$. (bottom row) El Niño $\langle\chi\rangle_{EN}$. The hatched contours indicate zones where χ is significant at 5%.

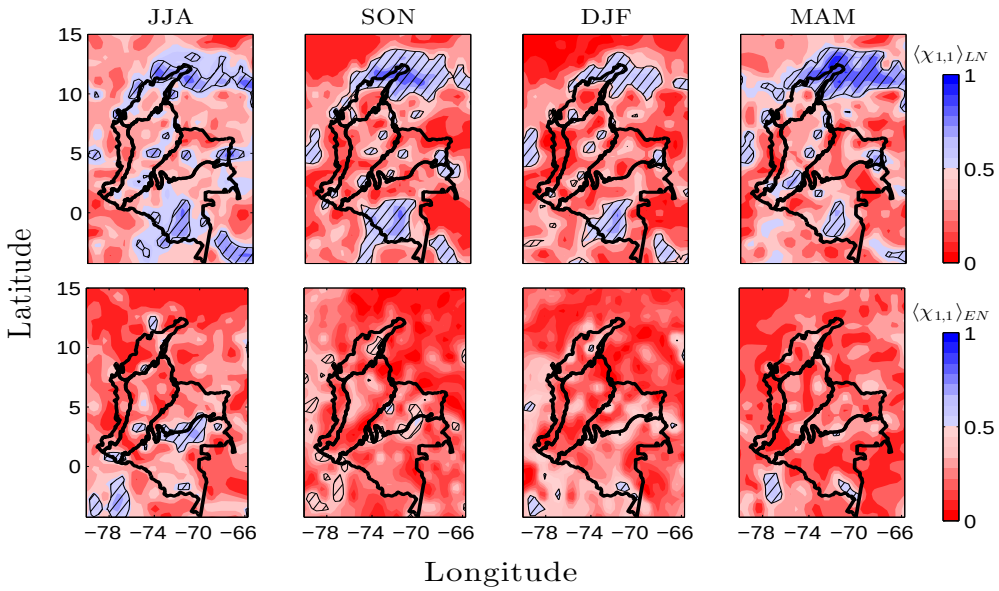

Figures B-22.: Strength of phase synchronization, $\langle\chi\rangle$, between the QBO index and rainfall anomalies in Colombia during ENSO. Phase ratio $\Phi_{1,1}$, Data set No. 1. (top row) La Niña $\langle\chi\rangle_{LN}$. (bottom row) El Niño $\langle\chi\rangle_{EN}$. The hatched contours indicate zones where χ is significant at 5%.

C. Supplementary Material – Chapter 4

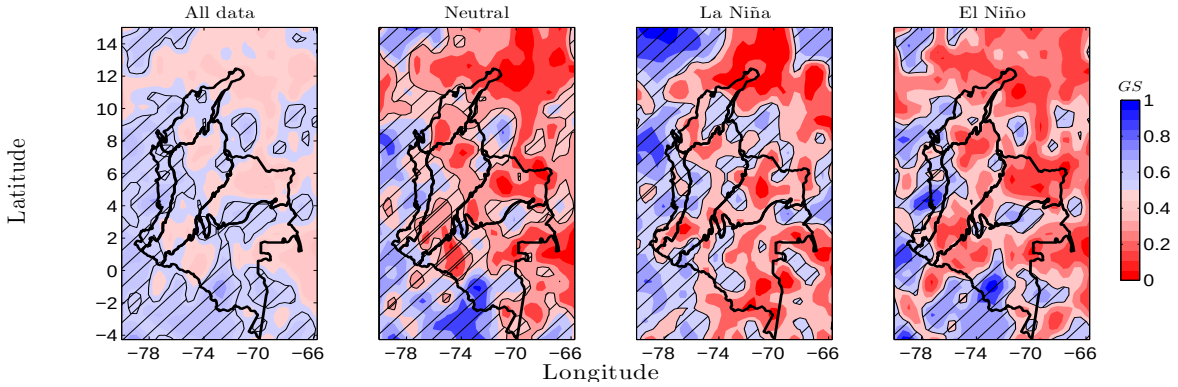

Figures C-1.: Generalized synchronization between SST gradient in the far-eastern Pacific and rainfall anomalies. Dataset No.1, period 1975-2006. The hatched contours indicates zones where the GS is significant at 5%.

Tables C-1.: XM river flow gauges, record length 1976–2015

ID	Latitude	Longitude	River	Dam	Central
1	3.53	-76.87	Alto Anchicaya	Alto Anchicaya	Alban
2	4.90	-73.30	Bata	Esmeralda	Chivor
3	2.71	-75.43	Betania	Betania	Betania
4	4.54	-74.26	Bogota	Agr.Bogota	Pagua
5	3.88	-76.56	Calima	Calima	Calima
6	2.94	-76.71	Cauca-Salvajina	Salvajina	Salvajina
7	4.57	-73.70	Chuza	Agr.Bogota	Pagua
8	6.51	-75.45	Grande	Riogrande	La Tasajera
9	6.78	-75.25	Guadalupe	Troneras	Guatron
10	6.29	-74.94	Guatape	Playas	Playas
11	4.73	-73.48	Guavio	Guavio	Guavio
12	5.56	-74.89	Miel I	Amani	Miel I
13	6.32	-75.17	Nare	Peñol	Guatapé
14	6.81	-75.15	Porce II	Porce II	Porce II
15	3.76	-74.89	Prado	Prado	Prado
16	6.21	-74.84	San Carlos	Punchina	San Carlos
17	6.39	-74.99	San Lorenzo	San Lorenzo	Joaguas
18	6.78	-75.32	Tenche	Miraflores	Guatrón

Tables C-2.: IDEAM river flows gauges, record length 1976–2013.

ID	IDEAM code	Name	River	Latitude	Longitude
0	1107701	Bellavista	Atrato	6.57	-76.57
1	1105702	San Padu Antonio	Atrato	6.28	-76.77
2	2306706	Tobia	Negro	5.13	-74.45
3	2308715	Pte Real	Negro	6.15	-75.38
4	2205704	Palmalarga	Saldana	3.68	-75.33
5	2619703	Remolino El	San Juan	5.87	-75.92
6	2119703	Playa La	Sumapaz	4.2	-74.5
7	2903702	Calamar	Magdalena	10.25	-74.91

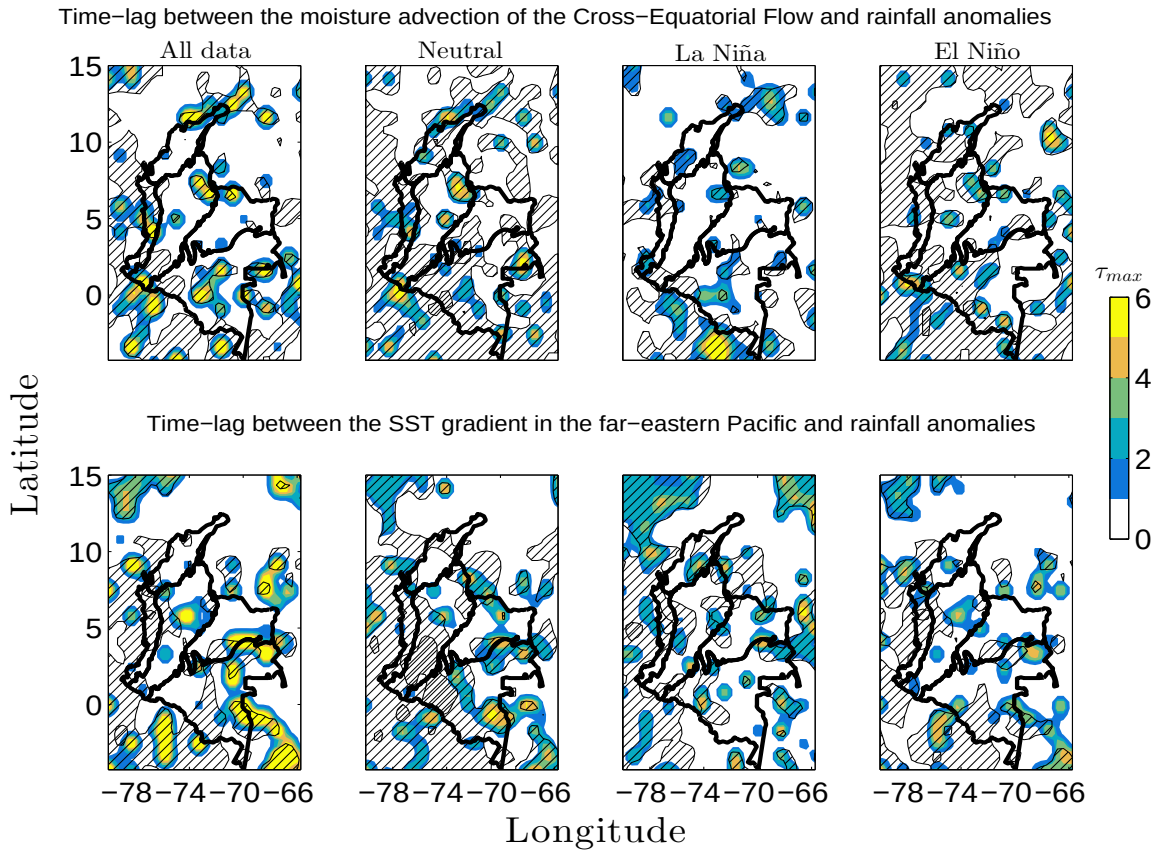

Figures C-2.: Time-lag in months between (top row) the moisture advection by the Cross-Equatorial Flow and rainfall anomalies and, (bottom row) SST gradient in the far-eastern Pacific and rainfall anomalies. Dataset No.1, period 1975-2006. The hatched contours indicates zones where the GS is significant at 5%.

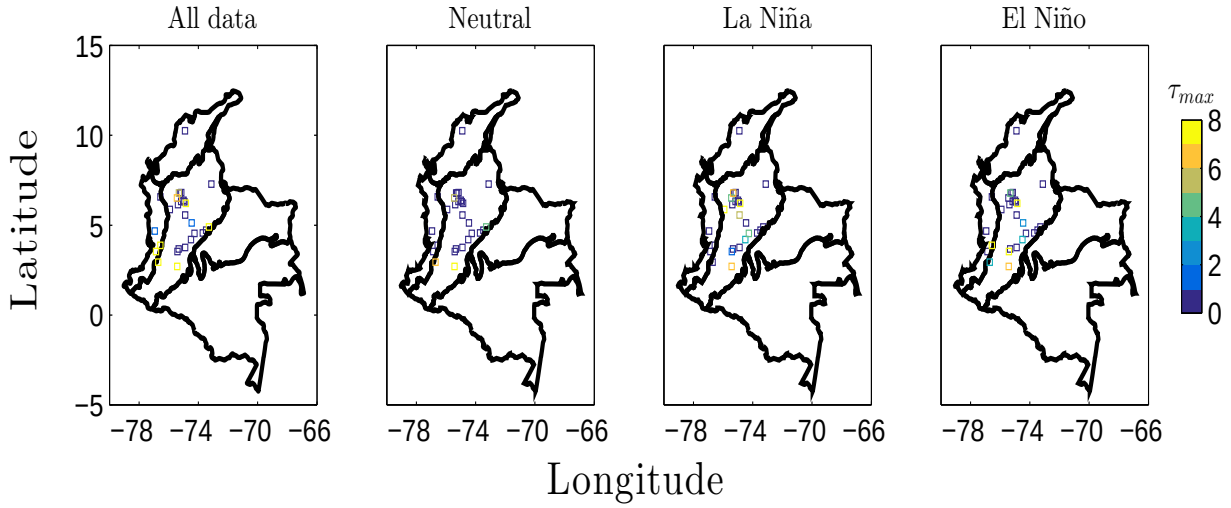

Figures C-3.: Time-lag in months between MEI and streamflows anomalies, period 1976-2013.

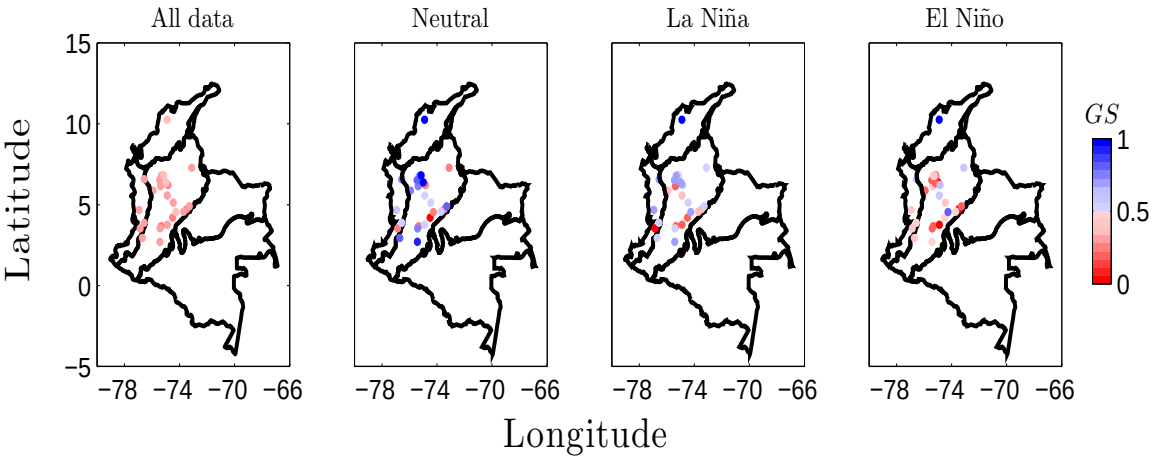

Figures C-4.: Generalized Synchronization Index between the Eastern Pacific (EP) index and river flow anomalies from the IDEAM and XM datasets, period 1976-2013.

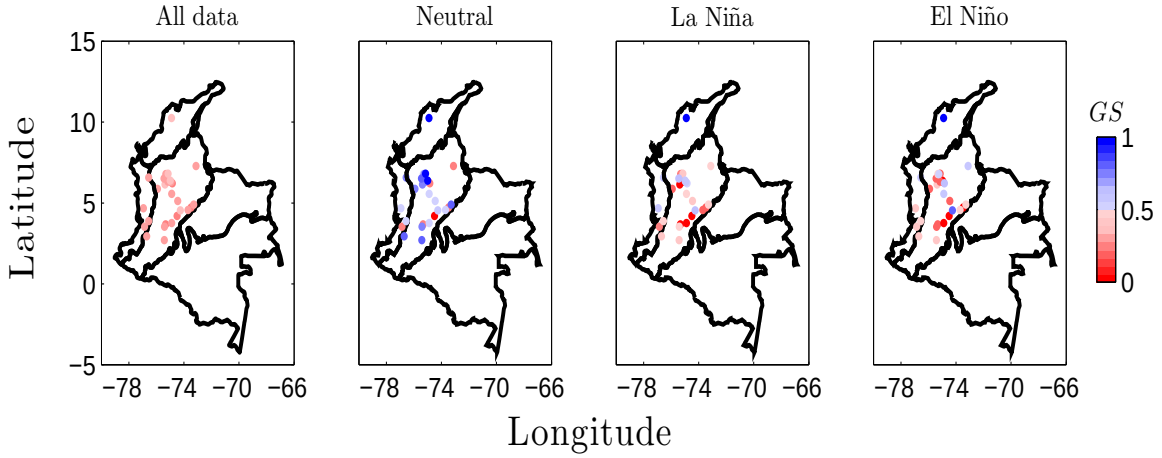

Figures C-5.: Generalized Synchronization Index between the Central Pacific (CP) index and river flow anomalies from the IDEAM and XM datasets, period 1976-2013.

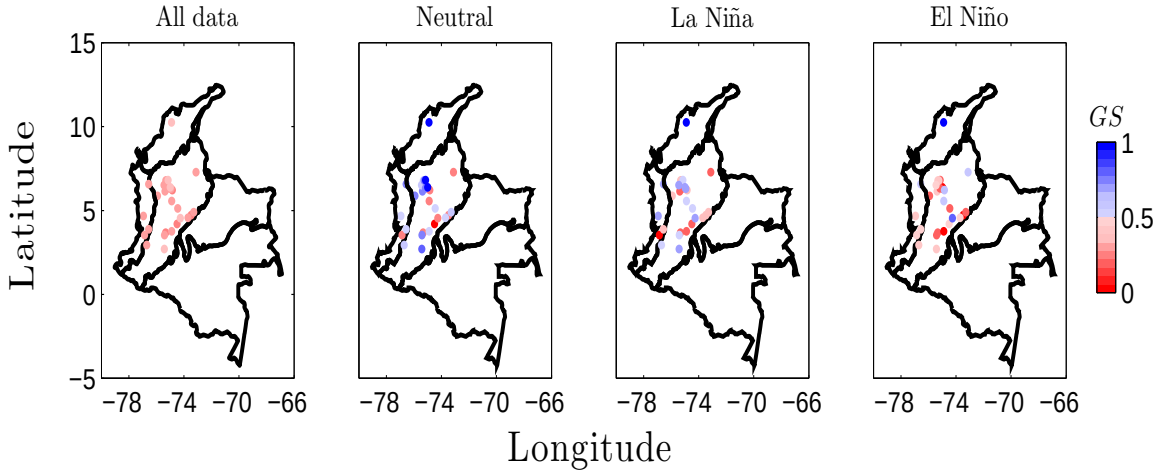

Figures C-6.: Generalized Synchronization Index between the Mixed-type index and river flow anomalies from the IDEAM and XM datasets, period 1976-2013.

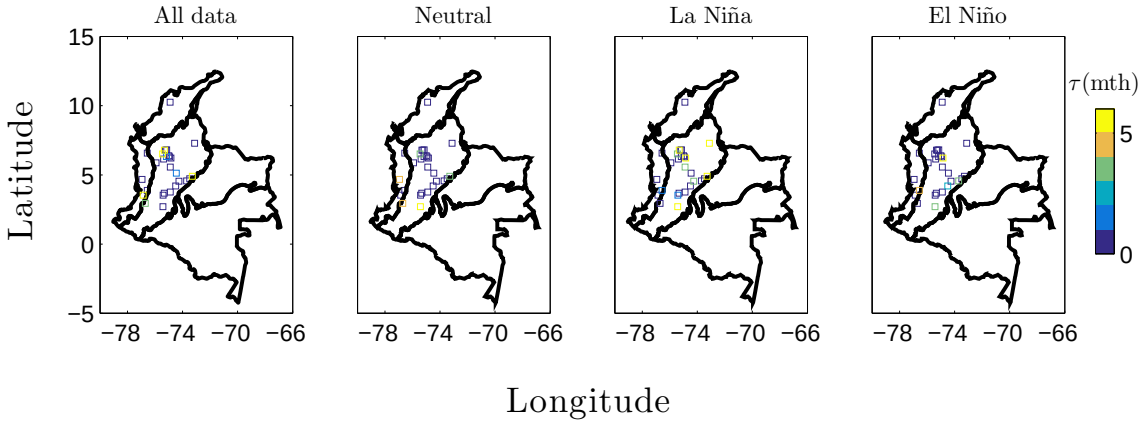

Figures C-7.: Timelags between the Eastern Pacific (EP) index and streamflow anomalies from the IDEAM and XM datasets, period 1976-2013.

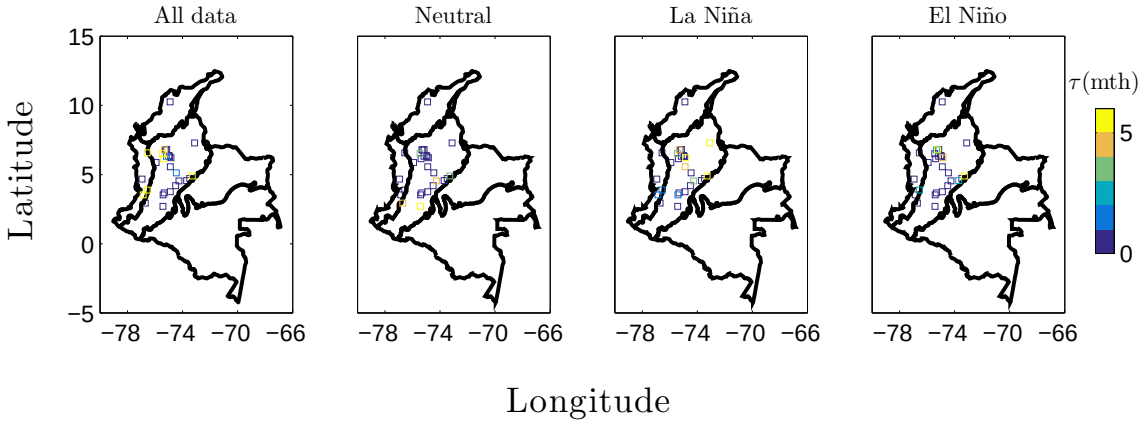

Figures C-8.: Timelags between the Central Pacific (CP) index and streamflow anomalies from the IDEAM and XM datasets, period 1976-2013.

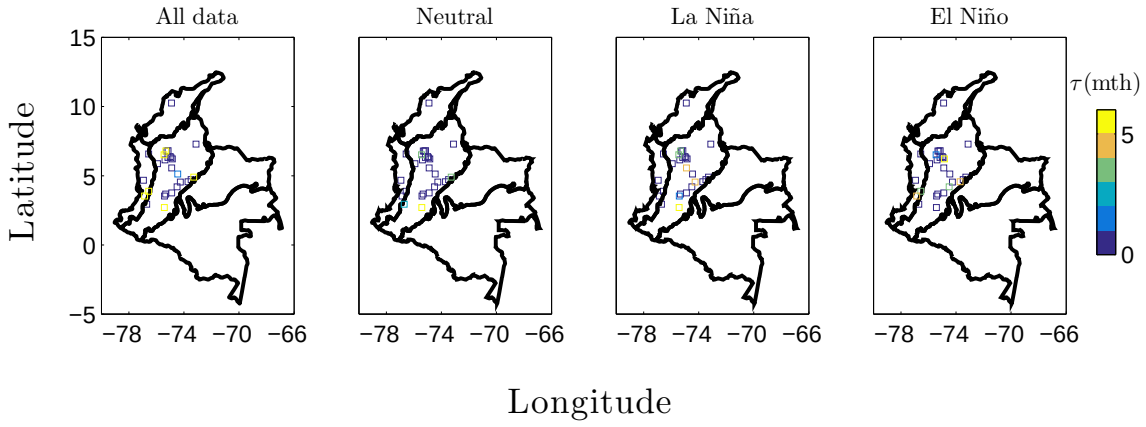

Figures C-9.: Timelags between the Mixed-Type El Niño index and streamflow anomalies from the IDEAM and XM datasets, period 1976-2013.

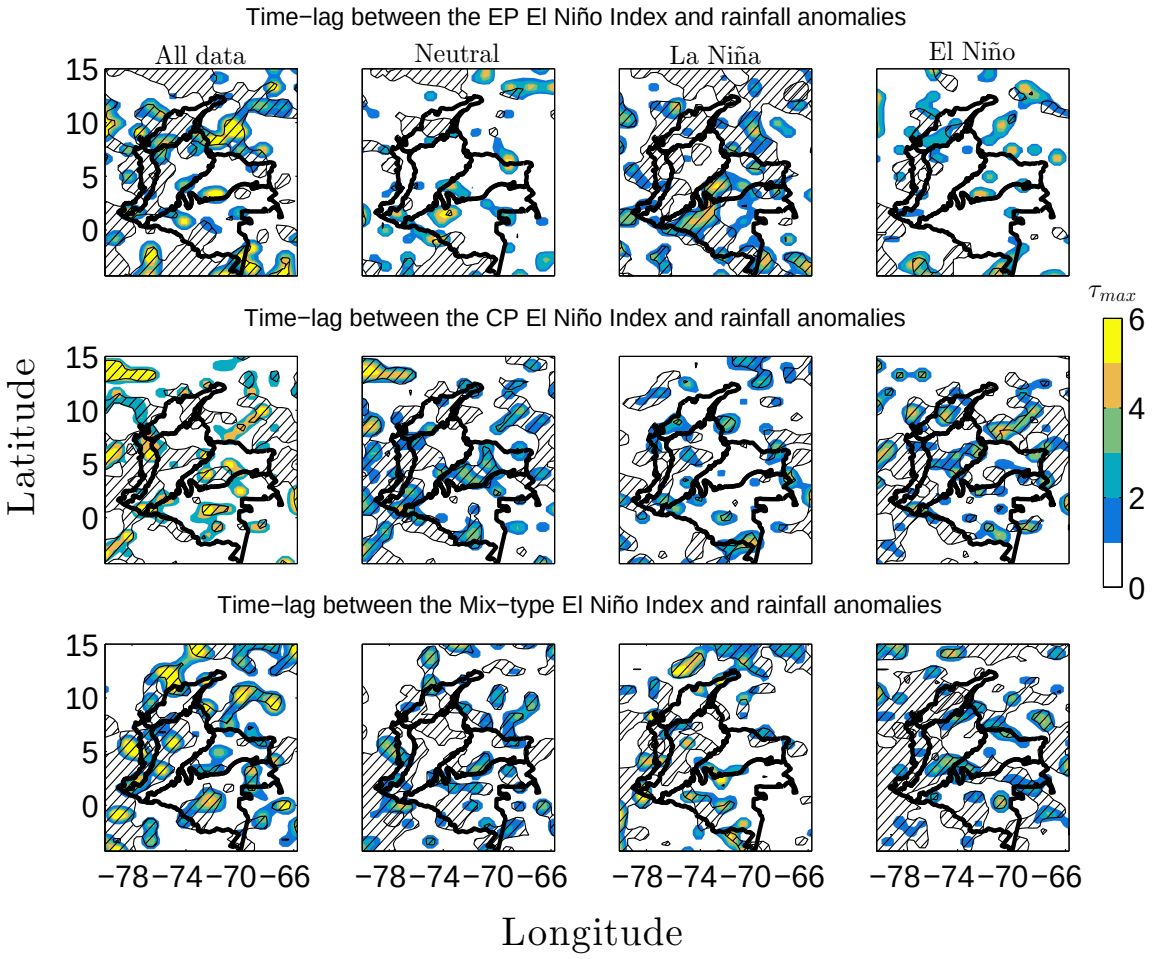

Figures C-10.: Time-lag in months between (top row) Eastern Pacific (EP) type of El Niño index and rainfall anomalies, (middle row) Central Pacific (CP) type of El Niño index and rainfall anomalies, and (bottom row) Mixed-type of El Niño index and rainfall anomalies. Dataset No.1, period 1975-2006. The hatched contours indicates zones where the GS is significant at 5%.

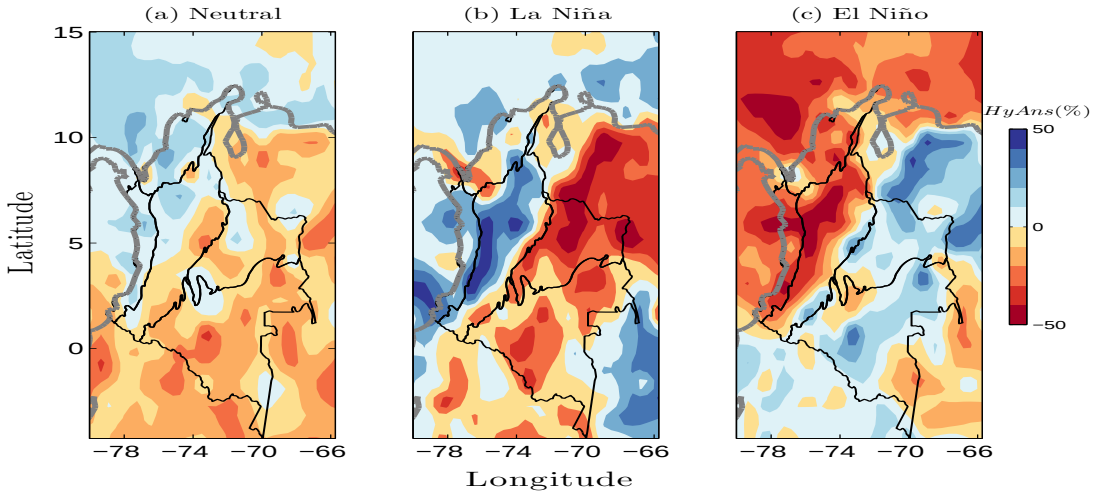

Figures C-11.: Composite average rainfall anomalies in Colombia during ENSO. Rainfall anomalies were calculated using F-Filtering of the annual cycle by moving averages, which is previously mentioned as the HyAns–FAC method. (gray line) northern South American coast line. (black line) Borders of the Colombia's natural regions.

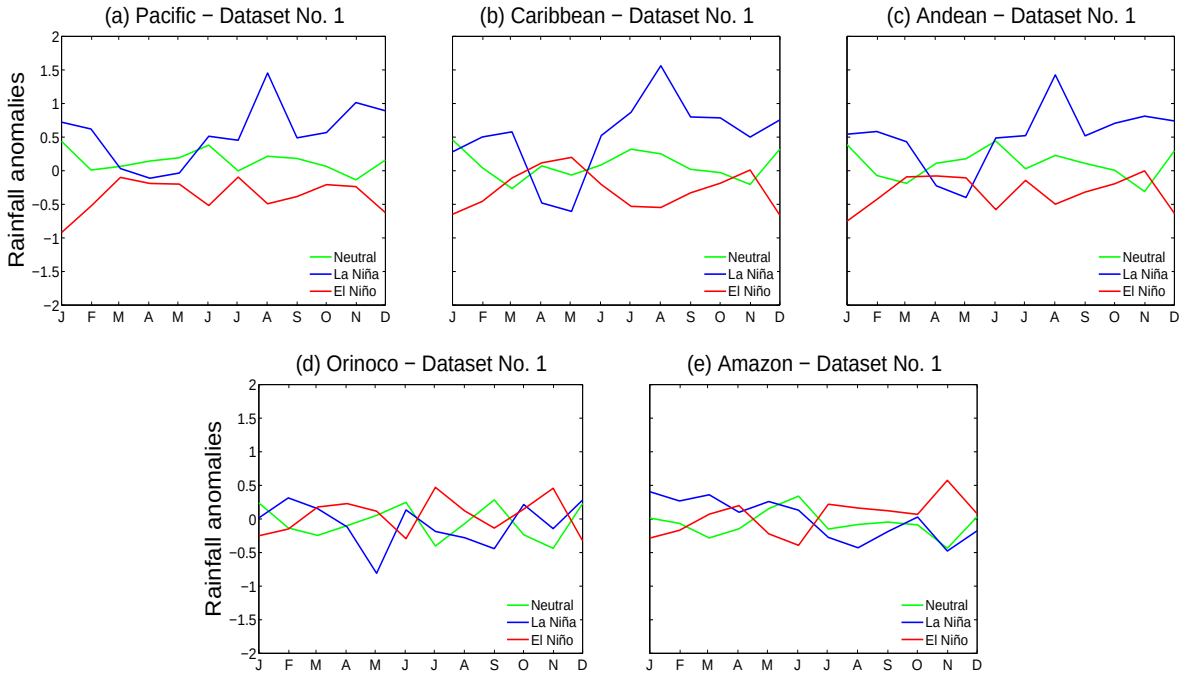

Figures C-12.: Annual cycle of rainfall anomalies averaged over the five natural regions (Pacific, Caribbean, Andean, Orinoco, and Andes) of Colombia during the phases of ENSO (La Niña, El Niño and Neutral) for Dataset No. 1, period 1975-2006.

Bibliography

[*Ahdesmäki, et al.*(2005)] Ahdesmäki, M., Lähdesmäki, H., Pearson, R., Huttunen, H., Yli-Harja,O. (2005) Robust detection of periodic time series measured from biological systems, *BMC Bioinformatics*, 6 (117), 1-18.

[*Hurtado and Mesa*(2014)] Hurtado-Montoya, A. and Mesa, O.J. (2014) Reanalysis of monthly precipitation fields in Colombian territory, *Dyna*, 81(186), 251-258.